`

Modular Gravitational Reference Sensor Development

Ke-Xun Sun, Saps Buchman, Robert Byer, Dan DeBra, John Goebel*, Graham Allen, John W. Conklin, Domenico Gerardi, Sei Higuchi, Nick Leindecker, Patrick Lu, Aaron Swank, Edgar Torres, and Martin Trittler

Hansen Experimental Physics Laboratory, Stanford University, CA 94305, USA
*Code RET, NASA Ames Research Center, Moffett Field, CA 94035, USA

kxsun@stanford.edu

Abstract. The Modular Gravitational Reference Sensor (MGRS) is targeted as a next generation core instrument for both space gravitational wave detection and an array of other precision gravitational experiments in space. The objectives of the NASA funded program are to gain a system perspective of the MGRS, to develop key component technologies, and to establish important test platforms. Our original program was very aggressive in proposing ten areas of research and development. Significant advancements have been made in these areas, and we have met or exceeded the goals for the program set in 2007-2008. Additionally, we have initiated research projects for innovative technologies beyond the original plan. In this paper we will give a balanced overview of progress in MGRS technologies: the two layer sensing and control scheme, trade-off studies of GRS configurations, multiple optical sensor signal processing, optical displacement and angular sensors, differential optical shadow sensing, diffractive optics, proof mass center of mass and moment of inertia measurement, UV LED charge management, proof mass fabrication, thermal control and sensor development, characterization for various proof mass shapes, and alternative charge manage techniques.

1. Introduction

The Modular Gravitational Reference Sensor (MGRS) [1-2] represents the next generation of technology for space gravitational wave detection and other space-borne gravitational precision experiments. MGRS will employ new technologies to achieve higher performance required for missions beyond LISA. MGRS also has a simpler structure and thus lower cost. We will use all-optical sensing to achieve near-zero stiffness. We will use two-layer interferometric and shadow sensing to maximize the fidelity of science measurement and to ease drag-free control. We will use a spherical proof mass to establish a full 3-dimemsional geodesic reference. We will use a larger gap between proof mass and housing to minimize the disturbances. We will take advantage the latest semiconductor technologies by using UV LEDs for charge management. We have demonstrated the exceptional radiation hardness and long operation life time of an UV LED. We are developing ground testing platforms for characterization of the mass center location and moment of inertia of the proof mass. We have designed and are building thermal environment control with microkelvin stability. Our program, funded by NASA, has more than ten technical areas. We have made significant advancements, and met or exceeded the aggressive goals for the effective funding period of June 2007

`

to March 2008. In addition, we have initiated research projects beyond the original plan. In this paper we will provide an overview of our progress.

2. MGRS Technologies

2.1. System Technologies

2.1.1. *Sphere and cube GRS overview (Collaboration with EADS Astrium)* [2] Collaborating with EADS Astrium, we have conducted a high level review [2] of the state of the art of the LISA GRS. We also started a trade study of GRS configurations with cubic proof masses or with a single spherical proof mass (MGRS). The results shows that the performance of the cubic proof mass configurations are adequate for the LPF baseline requirement. Further, the MGRS with a spherical proof mass holds promise as a future GRS, because of its simpler structure and higher performance at low frequencies.

2.1.2. *Sphere and cube trade-off studies: Noise tree (Collaboration with EADS Astrium)*[14] Stanford and EADS Astrium collaboratively studied the acceleration noise trees for the MGRS, and compared the results with the cubic GRS. The results show that the noise from environmental disturbances for the MGRS and cubic GRS are 8.5×10^{-16} m/s^2 and 10.5×10^{-16}m/s^2, respectively, and the stiffness induced noises are 0.4×10^{-16} m/s^2, and 2.8×10^{-16} m/s^2, respectively. Based on these first estimates, the spherical MGRS has ~28% lower total acceleration noise as a result of its large gap, full optical sensing, and no electrostatic actuation. The MGRS further enables simpler drag-free control.

2.1.3. *Two-layer sensing and control* [8] We have devised a two-layer optical sensing scheme, in which the science measurement is accomplished via picometer precision interferometric sensors, and the drag-free control signal is mainly obtained via large dynamic range shadow sensors. There is a substantial overlap region between the two sensing layers.

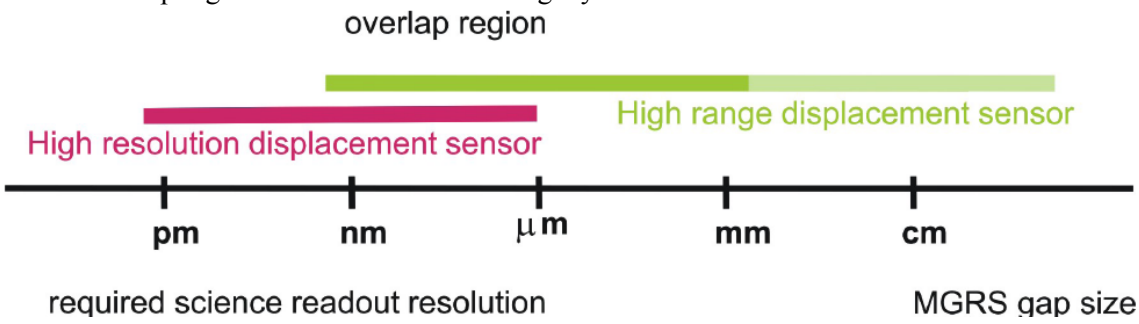

Figure 1. The two-layer sensing and control scheme. High precision laser interferometric sensors provide the science signal. High dynamic range optical shadow sensors provide the drag-free control signal. The two layers overlap in 0.1 nm-1 μm region.

2.1.4. *Mass center determination using multiple optical sensors* [3, 7, 8, 12, 13, 17]
We have undertaken an extensive set of analytical [12] and numerical [13] analyses to test the determination of the mass center position of a spinning sphere using a set of optical displacement sensors. The simulation demonstrates that we can accurately separate the proof-mass surface figure (~ 300 nm RMS) from its mass center motion (~ 30 nm RMS) using a numerical fit to the spin frequency and its harmonics. The simulation includes realistic system parameters such as sensor noise and residual drag-free error. The mass center displacement precision is better than 3 pm/Hz$^{1/2}$. This firmly establishes that a set of optical displacement sensors can be offer high precision and high system reliability.

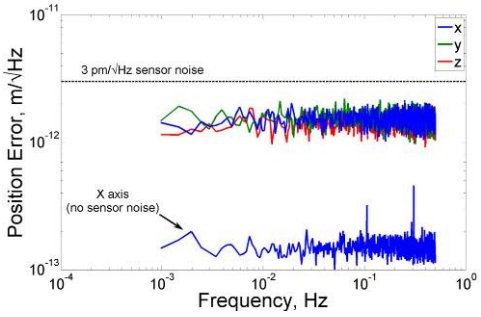

Figure 2: Simulation showing picometer determination of the mass center position, using multiple sensors. Head on sensors achieve even lower noise level (lower trace).

`

2.2. Optical Displacement Sensing [7, 8]

We have completed construction of a new test platform and vacuum chamber for the interferometric optical displacement sensor, consisting of a 900 line/mm grating, and a mirror surface simulating the proof mass. The cavity length is set at ~ 2 cm, resembling the gap size. The displacement signal is read out using a Pound-Drever-Hall RF modulation scheme. Preliminary testing in air on the new platform shows a noise level of 5 pm/√Hz at 1 Hz. The test platform will move into a vacuum chamber for improved performance.

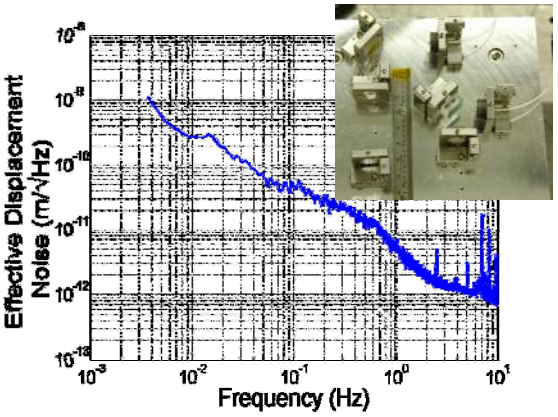

Figure 3. Preliminary results of the optical displacement sensor.

2.3. Differential Optical Shadow Sensing [7, 8, 19]

The Differential Optical Shadow Sensor (DOSS) scheme, shown in Figure 4, cancels laser intensity noise, while doubling the proof mass displacement signal. We have designed and constructed an optical shadow sensing test platform, on which the proof mass can be displaced with nanometer precision using a PZT driven flexure structure. We reduced the noise effects of electronics, electromagnetic interference, air flow and temperature, and achieved ~ 2 nm/Hz$^{1/2}$ at 2 Hz. The dynamic range is 1-3 mm, limited by the photodetector diameter. Our experience shows that optical shadow sensing is more robust than the interferometric sensors thanks to lower requirements in alignment and fringe counting. The method has been successfully applied to measurement of the mass center offset.

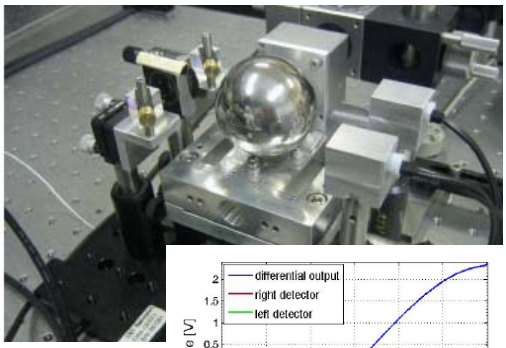

Figure 4: Shadow sensing test platform and calibration signal.

Figure 5.2: Sensor output over deflection

2.4. Optical Angular Sensing (Collaboration with Jet Propulsion Laboratory) [7, 8, 21]

We have improved the grating angular sensor by lowering noise and expanding the dynamic range. We have also constructed a vacuum enclosure for the entire grating angular sensor assembly. The photodetector and amplifier circuits now can receive higher laser power without saturation. With a mere working distance of 6 cm, and with an input laser power of 14 mW, we have observed an angular sensitivity of ~ 0.2 nrad/Hz$^{1/2}$ using the symmetric grating angular sensor. At low frequencies, we have achieved 1-2 nrad/Hz$^{1/2}$ at 1 Hz. The angular sensor will be applicable for both MGRS and space telescope steering.

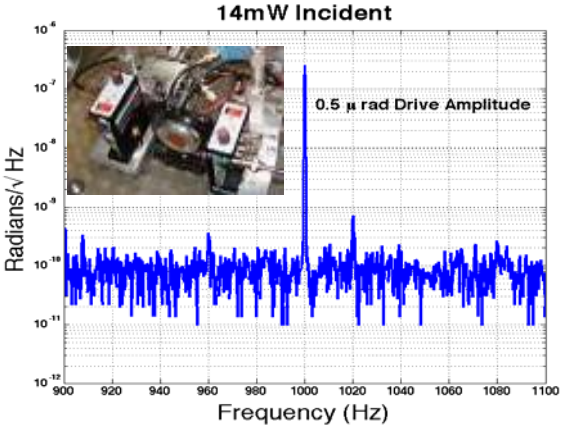

Figure 5. Measurement results from the grating angular sensor. The noise floor was below 2×10^{-10} rad/Hz$^{1/2}$. Inset: Grating angular sensor in vacuum chamber.

`

2.5. Diffractive Optics (Collaboration with Lawrence Livermore National Lab.) [18, 20]

We have expanded our diffractive optics work to characterize some LLNL gratings that may have applications in external interferometry, which requires high diffraction efficiency. We constructed grating cavities with extensive work in improving alignment, mechanical stability, interferometric calibrating the PZT actuation, and mode matching. Our highest observed finesse so far was 1002 ± 2.5, or a grating diffraction efficiency of 99.577 ± 0.002%. For higher power beam splitting applications, we tested the thermal characteristics of the dielectric gratings by illuminating a sample with up to 34.5 W of 1064 nm light in a 1.5 mm diameter spot without observing significant wavefront distortion with a Shack-Hartmann wavefront sensor.

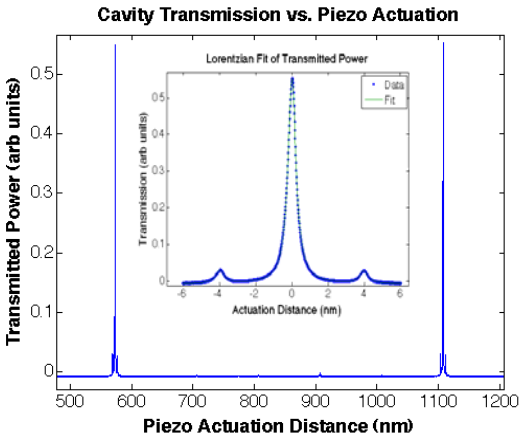

Figure 6. Grating cavity transmission versus cavity scan. Finesse of 1002 is demonstrated, representing diffraction efficiency of 99.577%. Inset: Blow up of the resonance portion.

2.6. Laser Frequency Stabilization Using a Grating Angular Sensor [7, 9]

The typical scheme for laser frequency stabilization utilizes a resonant optical cavity. Ambiguity in absolute frequency may occur due to periodicity in the cavity spectra. We propose to use the grating angular sensor as a non-resonant, robust laser frequency stabilizer. The grating angular sensor takes advantage of grating angular magnification and beam projection compression, thus exhibiting a high angular sensitivity of 0.1 nrad/$Hz^{1/2}$. The laser frequency deviation to produce such a small angle is ~ 300 kHz. Frequency stability at this level is sufficient for many practical applications, such as the absolute frequency indicator for LISA. In addition, the grating stabilizer will have a simpler structure and easier mechanical alignment.

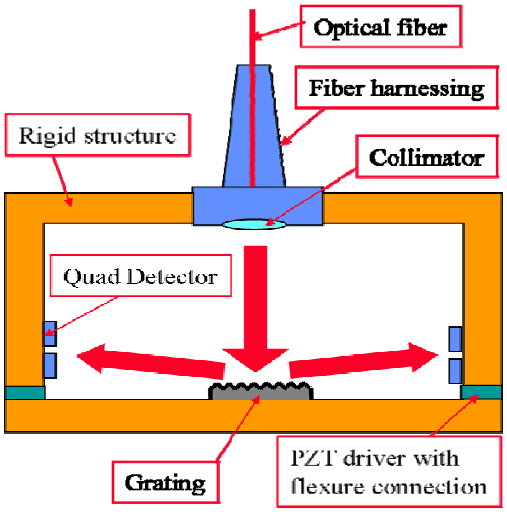

Figure 7. Structure of the grating laser frequency stabilizer

2.7. Center of Mass Measurement [7, 8, 22]

A new approach for measuring the mass center location of a spherical proof mass has been demonstrated to 150 nm precision. Knowledge of the mass center of a drag-free test mass is critical for calibrating the cross-coupling between rotational and translational degrees of freedom, and for inferring density inhomogeneities in the test mass material. In the past year, improvements in precision have come from the damping of mechanical vibrations due to the sphere rolling, careful isolation of the electronics to remove systematics caused by magnetic field fluctuations, shielding from air convection currents, and improving the detectors and data acquisition system design.

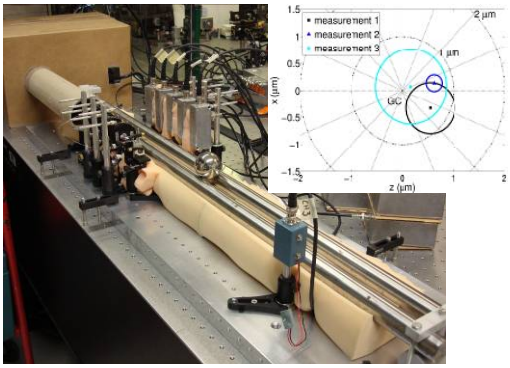

Figure 6. Mass center measurement apparatus, with improved vibration isolation and electronic noise reduction. Inset: Measurement of the mass center. Standard deviation < 150 nm.

`

2.8. Moment of Inertia and Self Gravity Attraction [16]

The five-wire torsion pendulum apparatus for moment of inertia measurements has been improved. A new version was designed and fabricated using SolidWorks CAD modelling software and a CNC milling machine. The improved design has a better mass balance and better tension distribution, resulting in reduced translational motion. In addition, a quad photo-detector was added to the grating angular sensor for higher sensitivity. The pendulum now can operate with higher spectral purity or signal to noise ratio. The amplitude spectral density plot shows a clean peak at the natural frequency around 3 Hz with error sources due to translation shifted above the measurement band.

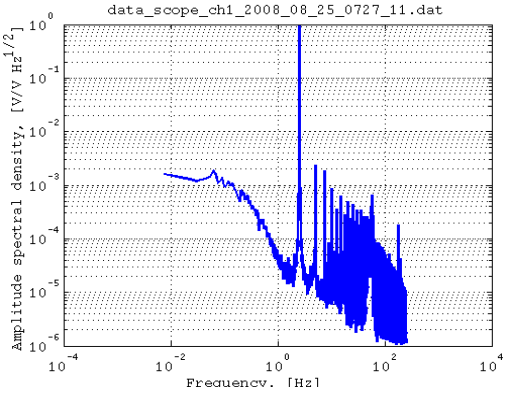

Figure 8. Spectrum from improved five wire torsion pendulum.

2.9. Proof Mass and Housing Fabrication [6][7][14]

Our efforts have focused on making a spherical test mass with preferred principal axis, accomplished using a TM with internally hollowed out portions and a spherical outer surface. For proof mass moment of inertia difference $\Delta I \geq 0.1I$ and a spin frequency > 10 Hz, the polhode frequency is > 1 Hz, above the science band of 0.1 mHz – 1 Hz. Fabrication of such a TM has been demonstrated using 50 mm diameter brass spheres with an average density loss < 20% [14]. Methods of lapping and polishing these spheres is under development with an ultimate goal of achieving an out-of-roundness < 100 nm.

Figure 9. Demonstration of assembly and lapping and polishing of 8 brass spheres with $\Delta I/I \sim 0.1$

2.10. Cubic Proof Mass Characterization [22]

In addition to developing the MGRS, our program is designed to help the LISA baseline configuration. We have designed several methods of measuring the mass center of a cubical proof mass. One technique would use our sphere mass center determination equipment with an internal kinematic mount for the cube inside a sphere which would have its mass center separated from the spherical holder mass center by reversal. A second method would use a torsion pendulum like apparatus shown in Fig. 10, but the cube would be offset a maximum distance from the center of rotation. The pendulum natural frequency depends quadratically on the distance between the mass center of the cube and the rotation axis. Mounted with its 4 major diagonals vertical there are 24 orientations of the cube in a triangular kinematic mount. Therefore, measuring the natural frequency with the cube in these various orientations allows us to accurately measure the cube's mass center. A third would develop a static pendulum with elastic hinges neutralized by a high mass center. A laser interferometer measures the neutral position of the pendulum. Reversal of the cubic mass on the triangular pendulum platform separates the mass center of the cube from that of the platform.

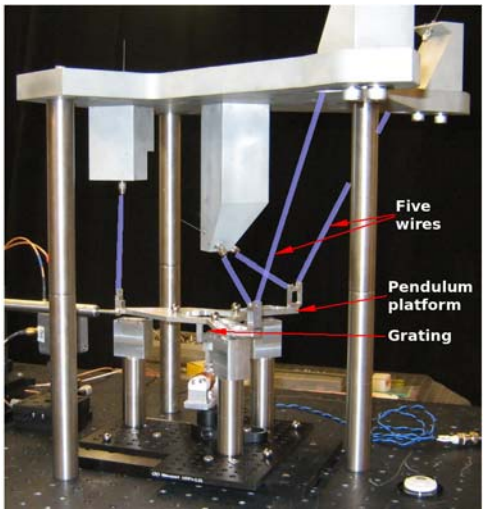

Figure 10. Five wire pendulum for proof mass characterization

`

2.11. UV LED Charge Management System [3][4][6][7][23]

We have continued UV LED power and spectral lifetime tests. The UV LED has now been operated more than 15,000 hours without significant power drop. The spectral shift is measured to be ~ 1 nm towards shorter wavelengths, which actually enhances photoelectric effects. Another power stability test has been initiated in a vacuum chamber several months ago. We have demonstrated that the UV LED is far superior to mercury lamps in reliability. Thus a UV LED based AC charge management system developed at Stanford should be the first choice for LISA and other high precision space flights requiring charge control.

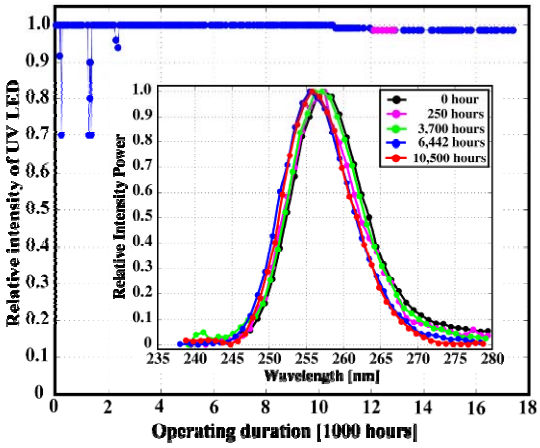

Figure 11. UV LED power and spectral stability.

2.12. UV LED Radiation Hardness Test [23]

We have conducted large dose radiation hardness tests using an accelerator source for 63 MeV protons. For proton fluence from 10^{10} to 10^{12} protons/cm^2, there was no significant power drop for UV LED light output at 255 nm wavelength. The UV emission spectrum also remains the same. This level of radiation test exceeded 100 years of radiation dose in the deep space LISA orbit. Therefore, we have demonstrated the extreme radiation hardness of UV LED. The combination of the successful tests in power lifetime, spectral stability, and radiation hardness have proven that UV LED should be primary choice for the charge management system for LISA and other high precision space flights.

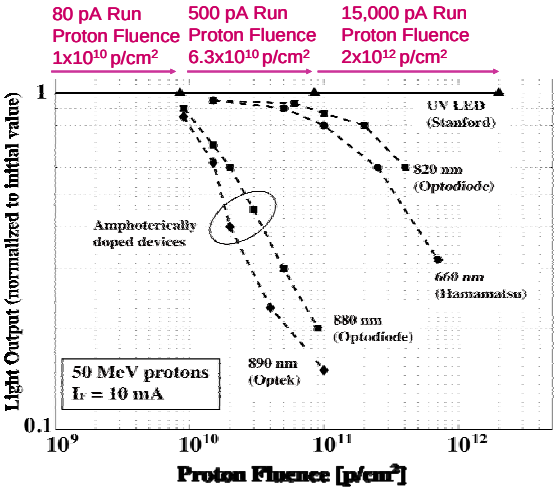

Figure 11. UV LED radiation hardness test. UV LED output power vs. proton fluence. Note: Data points other than UV LED are from Johnston et al. IEEE Trans. Nucl. Sci. p.2500 vol. 47 (2000).

2.13. Alternative Charge Management Scheme [11]

We proposed using ions and electrons of energy 1 eV–10 eV for neutralizing the charges on the non-conducting or isolated proof mass, which is possible for future GRS. By alternatively directing beams of positive and negative charges towards the mirror surfaces, we ensure the neutralization of the total charge as well as the equalization of the surface charge distribution. This method is compatible with operation in high vacuum, does not require measuring the potential of the mirrors and is expected not to damage sensitive optical surfaces.

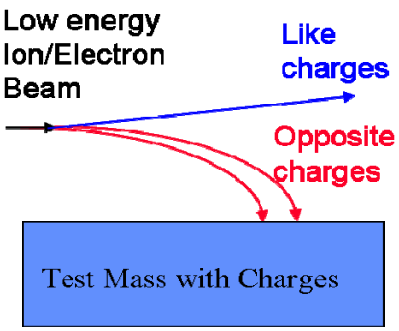

Figure 12. Charged particle neutralization for non-conducting surfaces.

`

2.14. Thermal Control [3] [24]

We are developing combined passive and active thermal control system with the goal of achieving sub microkelvin temperature stability and uniformity over a bench size volume. For the active control, we have developed a model predictive control (MPC) scheme, which will provide temperature controllability down to sub-microkelvin over the LISA science band. The very bottom of the curve in the Fig. 13 corresponds to the power spectral density of the new control law. For the passive control, we are designing a new thermal enclosure with multilayer structure with alternative conducting and insulating layers which insures the temperature uniformity and eases the burden on the active control. The upgraded thermal enclosure will be an important test facility for MGRS development. The stability of the new chamber is as low as 4 $mK/Hz^{1/2}$ at 1 mHz, which is a factor of 5 improvement over the insulation only enclosure. The uniformity improvement is expected to be even more significant.

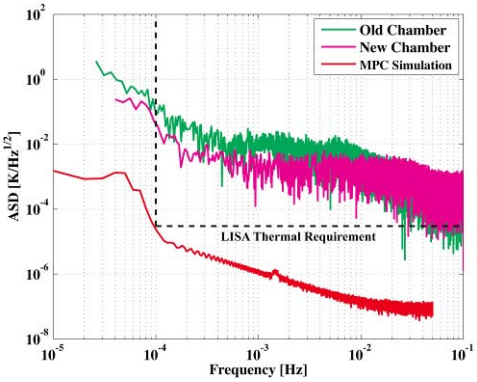

Figure 13. Results from model predictive controller model.

2.15. Temperature Sensor

We studied temperature sensor stability and resolution of multiple thermistors. Four thermistors were mounted to a common thermal block with adjustable temperature, and connected to Wheatstone bridges. Temperature cycles of ~ 1 mHz were applied during typical periods of 72 hours. Thermocouples were used for coarse readout calibration. Temperature data shows that the correlations between thermistor readouts are typically greater than 98%. Therefore, multiple thermistors can be used to enhance signal to noise ratio and redundancy, while maintaining adequate consistency.

Figure 14. Newly constructed multi-layer thermal chamber.

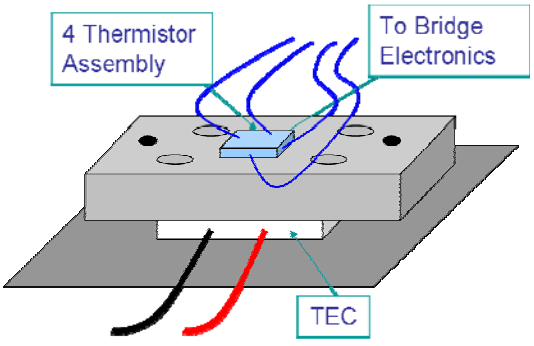

Figure 15. Thermistor, thermal couple (not shown), and TEC assembly for temperature sensor test.

3. Education and Science Outreach

The Stanford MGRS program has educated graduate, undergraduate, and high school students from diverse science and engineering backgrounds.

4. Conclusion

Our MGRS research has made significant progress in many key areas, in both enhancing the performance of the experiments and inventing new technologies. MGRS will contribute future precision gravitational space measurements.

Acknowledgements

This research was partially supported by NASA Beyond Einstein Foundation Science, Grant NNX07AK65G, for "Modular Gravitational Reference Sensor for Space Gravitational Wave Detection". We gratefully acknowledge the collaboration from Lawrence Livermore National Laboratory. The grating angular sensor research was funded by Jet Propulsion Laboratory.

`

References

[1] Ke-Xun Sun, G. Allen, S. Buchman, D. DeBra, and R. L. Byer, "Advanced gravitational reference sensor for high precision space interferometers", Class. Quantum Grav. 22 (10), S287 (2005).
[2] Ke-Xun Sun, Ulrich Johann (EADS Astrium), Dan B. DeBra, Sasha Buchman, and Robert L. Byer, "LISA Gravitational Reference Sensors," Journal of Physics CS 60 272–275 (2007).
[3] K.-X. Sun, S. Buchman, R. L. Byer, G. Allen, J. W. Conklin, D. DeBra, S. Higuchi, N. Leindecker, P. Lu, A. Swank, M. Trittler, "Technologies for an Advanced Modular Gravitational Reference Sensor," 18th International Conference on General Relativity and Gravitation, Sydney, Australia (2007).
[4] K.-X. Sun, N. Leindecker, S. Higuchi, S. Buchman, R. L. Byer, J. Hines, J. Goebel, E. Agasid, "Development of UV LED Based AC Charge Management Systems For Gravitational Wave Detectors," 7th Edoardo Amaldi Conference on Gravitational Waves, Sydney, (2007).
[5] Sasha Buchman, "Overview of GP-B Charging Issues" 2007 Workshop on Charging Issues in Experimental Gravity, Massachusetts Institute of Technology, July 26-27, (2007).
[6] Ke-Xun Sun, "UV LED AC Charge Management System for LISA and LIGO," Workshop on Charging Issues in Experimental Gravity, MIT, July 26-27, (2007).
[7] K.-X. Sun, S. Buchman, R. L. Byer, G. Allen, J. W. Conklin, D. DeBra, S. Higuchi, N. Leindecker, P. Lu, A. Swank, E. Torres, M. Trittler, "Technology Advances for LISA GRS and MGRS," LISA Science and Technology Team (LIST) Working Group 3 (DRS) Meeting, ESTEC, September (2007).
[8] Ke-Xun Sun for Stanford Team, "Progress in Optical Measurements for Science Signal and Spacecraft Control," LIST WG 2 (Interferometry) Meeting, ESTEC, September (2007)
[9] Ke-Xun Sun, Patrick Lu, and Robert Byer, "Laser Frequency Stabilization Using Diffractive Angular Sensors, Laser Science," Laser Science XXIII / OSA Frontier in Optics, San Jose, September (2007).
[10] S. Higuchi, D. B. DeBra, and S. Rock, "Sub-microkelvin Precision Thermal Control System Using Model Predictive Algorithm for Laser Interferometer Space Antenna (LISA) Ground Verification Facility", presented at the 22nd Annual ASPE Meeting, Dallas, Texas, October 14-19, (2007).
[11] S. Buchman, R. L Byer, D. Gill, N. A. Robertson, and K-X Sun, "Charge neutralization in vacuum for non-conducting, and isolated objects using directed low-energy electron and ion beams," Class. Quantum Grav. 25 035004 (2008).
[12] J. W. Conklin, G. Allen, K.-X. Sun, D. B DeBra, "Determination of Spherical Test Mass Kinematics with a Modular Gravitational Reference Sensor", AIAA J. Guidance, Control & Dynamics (2008).
[13] G. Allen, J. W. Conklin, K.-X. Sun, D. B. DeBra, R. L. Byer "Mass Center Position Determination of a Spinning Sphere as part of a Modular Gravitational Reference Sensor," to be submitted to AIAA Journal of Guidance, Control and Dynamics (2008).
[14] D. Gerardi, G. Allen, J. W. Conklin, K.-X. Sun, D. DeBra, S. Buchman, P. Gath, R. Byer, U. Johann, "Achieving Disturbance Reduction for Future Drag-Free Missions," to be submitted to CQG (2008).
[15] J. W. Conklin, D. Clark, M. Dreissigacker, M. Dolphin, M. Trittler, M. Ulman, and D. DeBra, "Fabrication of a Spherical Test Mass with a Preferred Principal Axis," in preparation (2008).
[16] Ke-Xun Sun, Saps Buchman, Graham Allen, Robert Byer, John Conklin, Dan DeBra, Sei Higuchi, Nick Leindecker, Patrick Lu, Aaron Swank, Edgar Torres, Martin Trittler, "Advances in Modular Gravitation Reference Sensor (MGRS) Technologies," 37th COSPAR, Montreal (2008).
[17] John W. Conklin, Graham Allen, Ke-Xun Sun, Saps Buchman, Robert L. Byer and Dan B. DeBra, "Modeling and Simulation of a Spinning Spherical Test Mass for Modular Gravitational Reference Sensor," 37th COSPAR, Montreal (2008).
[18] P. Lu, K.-X. Sun, R. L. Byer et al "Characterization of large size, high efficiency dielectric gratings," to be submitted to Optics Letters (2008).
[19] K.-X. Sun, M. Trittler, J. W. Conklin, R. L. Byer, "Differential Optical Shadow Sensing (DOSS) for LISA and MGRS Applications", 7th LISA Symposium (2008) (J. Physics C. This issue.)
[20] K-X. Sun, P. Lu, and R. L. Byer, "Characterization of High Efficiency Dielectric Gratings for Formation Flight Interferometry", *ibid*
[21] K.-X. Sun, P. Lu, and R. L. Byer ,"Grating Angular Sensor for LISA and MGRS Applications", *ibid*
[22] J. W. Conklin, A. Swank, K.-X. Sun, and B. DeBra, "Mass Properties Measurement for Drag-free Test Masses" *ibid*
[23] K.-X. Sun, N. Leindecker, S. Higuchi, S. Buchman, J. Goebel, R. L. Byer, "UV LED Operation Lifetime and Radiation Hardness Qualification for Space Flight", *ibid*
[24] S. Higuchi, K.-X. Sun, D. B. DeBra, S. Buchman, R. L. Byer, "Design of a Highly Stable and Uniform Thermal Test Facility for MGRS Development", *ibid*